

# 42-Volt Electric Air Conditioning System Commissioning and Control For a Class-8 Tractor

Bapiraju Surampudi, Mark Walls, Joe Redfield, Alan Montemayor  
Southwest Research Institute

**Chips Ingold**  
Modine Manufacturing

**Jim Abela**  
Masterflux

Copyright © 2003 SAE International

## ABSTRACT

The electrification of accessories using a fuel cell as an auxiliary power unit reduces the load on the engine and provides opportunities to increase propulsion performance or reduce engine displacement. The SunLine™ Class 8 tractor electric accessory integration project is a United States Army National Automotive Center (NAC™) initiative in partnership with Cummins Inc., Dynetek™ Industries Ltd., General Dynamics C4 Systems, Acumentrics™ Corporation, Michelin North America, Engineered Machine Products (EMP™), Peterbilt™ Motors Company, Modine™ Manufacturing and Masterflux™. Southwest Research Institute is the technical integration contractor to SunLine™ Services Group.

In this paper the SunLine™ tractor electric Air Conditioning (AC) system is described and the installation of components on the tractor is illustrated. The AC system has been designed to retrofit into an existing automotive system and every effort was made to maintain OEM components whenever modifications were made. Hardware modifications were limited to replacing the engine driven compressor for a 42 volt DC driven one, exchanging the expansion orifice for a thermal expansion valve and positioning the components to minimize the length of refrigerant lines.

The thermodynamics and PID control algorithms are discussed. Closed loop test results are presented in controlled ambient conditions. Analysis of reversed Carnot cycle changes due to transient operation and coefficient of performance changes are given.

## INTRODUCTION

The engine driven air conditioning system on the 2002 Peterbilt™ 385 is used for maintaining a comfortable in-cab temperature and as a windshield defroster. The Original Equipment Manufacturer (OEM) system includes a Sanden™ SD7 engine driven compressor that draws approximately 6 kW at full load. One disadvantage of this compressor is that it is the same one that is used on all of their trucks, and therefore it is sized for the trucks with the full size sleeper. Peterbilt™ and Modine™ engineers have designed this system to provide up to 25000 BTU/hr of cooling. Other disadvantages of having the engine driven compressor include constant parasitic losses from clutch drag, inability to operate the compressor in its efficient zones, and packaging.

## BASICS

### Block Diagram

The block diagram of the air conditioning system is shown in Figure 1. The locations of instrumentation of different parameters are shown in this figure. Two pressures (Compressor Outlet after condenser and compressor inlet or evaporator outlet) and six temperatures were measured for purposes of analysis and control. The state of the refrigerant at compressor inlet is named as 1, at compressor outlet as 2, at condenser outlet as 3 and evaporator outlet as 4.

### Objectives

The objectives of this paper are to present the preliminary steps involved in installing and commissioning an electrical air conditioning system.





Figure 2 SwRI™ Rapid Prototyping Electronic Control System (RPECS™) is used to control the 42 V AC System

### RPECS

The RPECS™ has a convenient PC/104 form factor with compact packaging for shorter wiring harness lengths while retaining full desktop processing power. It uses QNX 4.25 a hard real-time POSIX compliant operating system capable of supporting preemptive multitasking. The AC control software was developed using ANSI C. RPECS™ is RS232/RS485 compatible and can communicate using TCP/IP, CAN J1939 protocol, or MODBUS protocol. It has a built in UPS to handle voltage drop during cranking of the engine. It can tolerate supply voltage changes from 8 to 32 V DC. It can also operate between -25 to 60 deg C ambient temperatures. A single FPGA provides flexible digital I/O, logic and capability to measure/send PWM signals. The Graphical User Interface is installed on a laptop running Redhat™ Linux capable of communicating with QNX™ RTOS using TCP/IP. The hardware is easily extendible to accommodate required analog inputs/outputs and digital inputs/outputs.

### CONTROL BLOCK DIAGRAM

The block diagram for preliminary control system developed for commissioning of the AC system is shown in Figure 3. This system is to ensure that driver demanded cab temperatures are feasible with the components picked under controlled ambient conditions. It consists of a proportional integral controller that takes the error between driver desired cab temperature and actual cab temperature as input and produces a compressor speed set point command as an output.

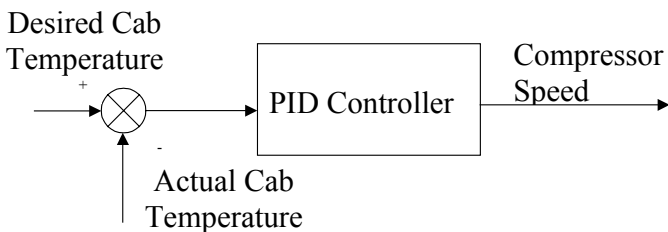


Figure 3 Preliminary AC Control System

### Test Results

The cab doors were closed and an external fan was blowing across the radiator for simulating airflow during truck movement. The closed loop test results are shown in the following figures. The PID controller was tuned for stability and steady state error of  $\pm 1$  °C. Two-step inputs in desired cab temperature were given and response of actual cab temperature is shown in Figure 4.

The compressor command from the PID controller and the power consumption (kW) of the compressor are shown in Figure 5. We can notice that as the desired temperature is achieved the compressor goes to its minimum setting of 1V. We can see that peak compressor power consumption is 1.5 kW and steady state consumption is 1 kW.

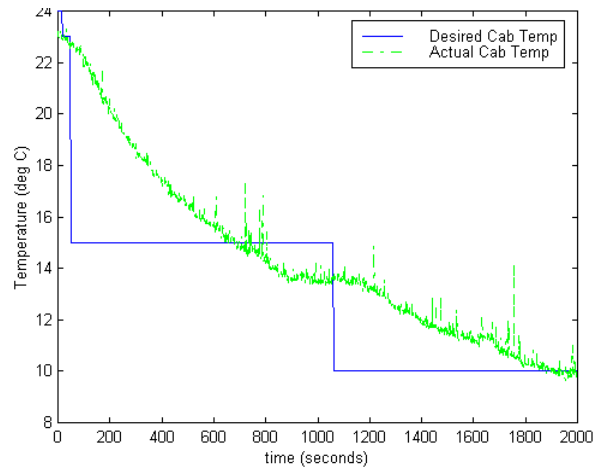


Figure 4 PID Controller Performance to Step Changes in Desired Cab Temperature

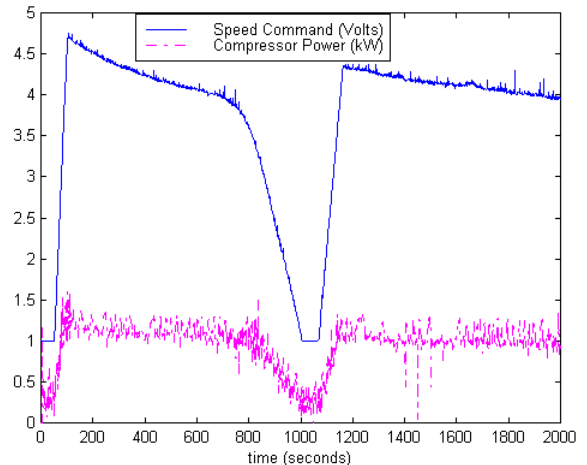


Figure 5 Compressor Command and Power commanded by the PID controller

The pressures across the compressor are shown in Figure 6. We can note that the inlet pressure goes up while the outlet pressure falls during initial portion of the step change. The oscillations observed are due to the expansion valve hunting. Corresponding temperature

effects are shown in Figure 7. The valve expansion valve orifice has been set to maintain a superheated 6.5 °F (or 3.5°C) at compressor inlet and its hunting (Figure 8) with respect to the superheated temperature (difference between Compress inlet temperature and corresponding saturated temperature). This hunting is seen normally in automobile A/C systems with variable valve orifice feedback.

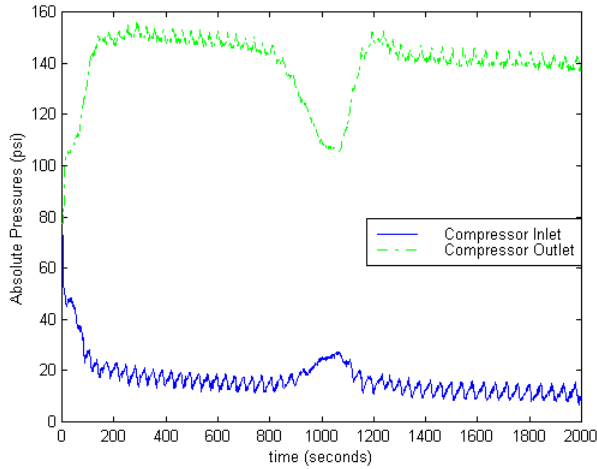


Figure 6 Compressor Inlet and Outlet Pressures (Not the oscillations due to expansion valve hunting)

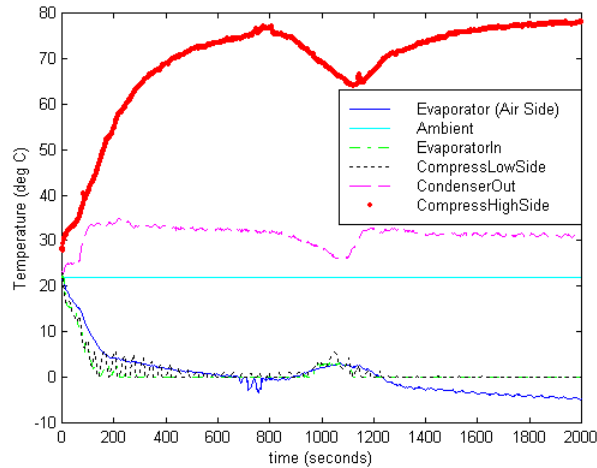


Figure 7 Temperature Variations during tracking of desired cab temperature

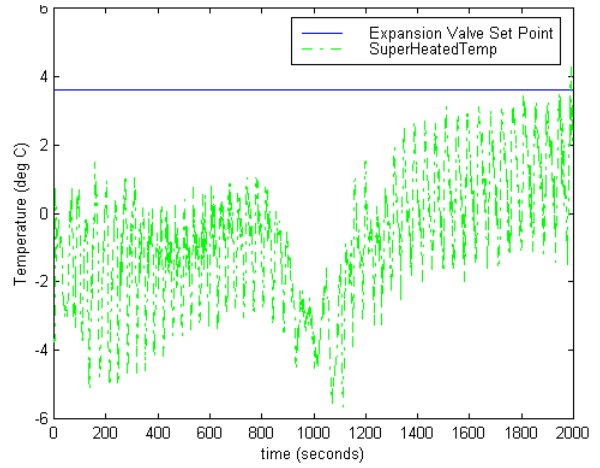


Figure 8 Expansion Valve hunting during attempts to achieve the superheat set point of 3.6 °C (6.5 °F) at Compressor Inlet

## ANALYSIS

The reverse Carnot cycle is shown in Figure 9. State 1 is compressor inlet, State 2 compressor outlet, 3 is expansion valve outlet and 4 is evaporator inlet. The expansion valve has been assumed to have adiabatic pressure drop and the pressure drops across the condenser and evaporator have been neglected. The enthalpies have been suitably calculated based on whether the refrigerant is superheated, subcooled or two phase mixture. The two thick magenta lines are liquid to vapor and vapor to liquid conversion points. The cyan blue lines are constant temperature lines in the superheated region. The cycle is plotted just for the first step response input. The cycle lines that are red and thin are for the beginning of step response and the lines that are blue and thick are for steady state or end part of the response. The color and line thickness progresses smoothly between the two extremes. We can notice that area is much higher in the transient region and smaller at steady state. The superheated point at state 1 scatters due to the expansion valve hunting and can be improved to stay closer to 6.5°F by tuning the orifice set point and the thermal inertia of the evaporator. Pinching off additional lines on the evaporator can change the thermal inertia. We can compute from the deviation of the process of compression (1 to 2) from isentropic line, the average operating compressor efficiency is about 60%.

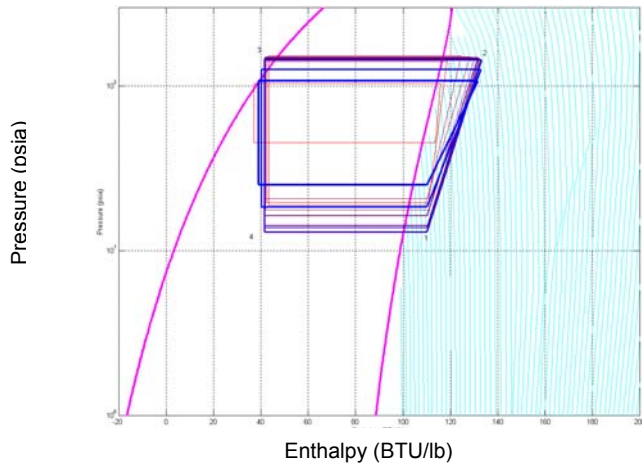


Figure 9 Reverse Carnot Cycle Variation during transient associated with first step change

The process for second step is shown in Figure 10. We can notice that significant additional work for the second step due to the low temperature set point (or the cold region in theoretical reverse Carnot cycle). These maps point to the targeted tuning of the AC system for improving the operating efficiency and are useful tool during commissioning of the system. The Coefficient of performance (COP) is plotted in Figure 11. The constant pressure drop assumptions and electrical sensor noise cause an actual COP to be slightly higher than the theoretical Carnot COP during initial transient. During steady state the COP converges to 2.8 compared to the possible theoretical COP of 3.2.

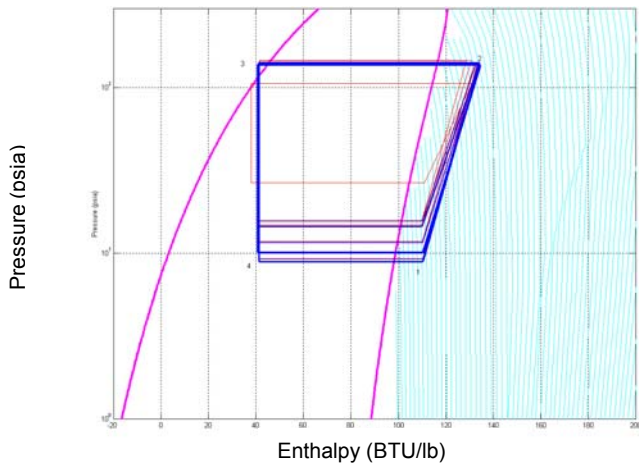


Figure 10 Reverse Carnot Cycle Variation during transient associated with second step change

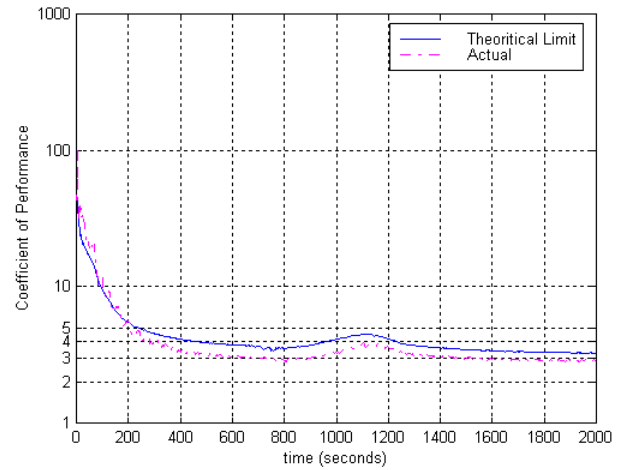


Figure 11 Coefficient of performance of the 42V AC System (2.8) is close to the theoretical limit (3.3)

## CONCLUSION

The 42 V electrical AC system has been installed in a Class 8 tractor and commissioning has been completed. Preliminary control strategies and analysis tools indicate promising areas of tuning the hardware and controller for minimizing the energy consumption of the system.

Although the present work is using a Class 8 tractor platform the approach and technique is generic enough for all classes of passenger automobiles. With clear indications of improvement in emissions and fuel economy with fuel cells and the convergence of the auto industry towards a 42 V electric system the two technologies are synergistic. Hybrid vehicles using electrification of accessories with a small fuel cell and the resulting reduction of engine size can pave the way for full-fledged fuel cell vehicles of the future.

Future work will target optimization of the AC system and developing mathematical models for exploring model based control strategies.

## ACKNOWLEDGMENTS

The authors would like to thank the SunLine™ Services Group, The United States Army National Automotive Center (NAC™), Cummins Inc., Dynetek™ Industries Ltd., General Dynamics C4 Systems™, Acumentrics Corporation™, Michelin North America™, Engineered Machine Products™ (EMP), Peterbilt™ Motors Company, Modine™ Manufacturing and Masterflux™ for their contributions to the Sunline integration project.

## REFERENCES

1. Michael J. Moran and Howard N. Shapiro, "Fundamentals of Engineering Thermodynamics", John Wiley and Sons Inc, New York.
2. Dupont SUVA Technical Information Publication T134a-ENG, "Thermodynamic Properties of HFC-134a"